Modeling and Simulation of an Active Heave Compensated Draw-works

Ahmed A.Walid, Peter Gu, Michael Rygaard Hansen, Geir Hovland and Yousef Iskandarani

Abstract—The following work is about the modeling, simulation and optimal designingof an activeheave compensation (AHC) system for a draw-works on a hoisting rig.Optimization of design parameters for such systems can be done by analyzing modelsimulations. To achieve this, ahydro-mechanical concept comprising the main components of the draw-works and hoisting rig were modeled. This model was implemented in simulation software "SimulationX" and tested for its dynamic performance in two load cases:vertical stabilization and gentle lowering to the seabed, both while under the influence of a sinusoidal wave. Thesimulation results revealed potential improvements in terms of the design parameters.

Keywords—Active heave compensation (AHC), draw-works, hoisting rig, modeling, simulation.

I. INTRODUCTION

THE operation of hoisting machinery out at sea poses the problem of wave induced heave motion interfering with the positioning of a payload.This problem exists in 6 degrees of motion, but heave motion is the most problematic. Motion interference also causes great variationsin the forces transferred to a mechanical hoisting system which may cause structural damage. Thus, hoisting operations can not be carried out in wavy sea conditions.

Over the years, both passiveheave compensation (PHC) and active heave compensation systems (AHC) have been researched and developed in order to lessen this problem. Examples of research on PHC systems include the work by Driscoll et al. who found stiffness and damping characteristics of a passive cage-mounted heave compensator [1]. Another work on PHC is by J. Ni et al. who proposed a PHC system with accumulators [2].

PHC systemsare useful due to their practicality in terms of cost and design compared with AHC systems. PHC systems have ca. 85% efficiency in heave compensation when ship heave is > ~4m, but only ca. 40% when ship heave is < ~2m

Ahmed. A. Walid is with the Department of Engineering, Faculty of Engineering and Science, University of Agder, N-4898 Grimstad, Norway (e-mail: walid@student.uia.no).

Peter Gu is with the Department of Engineering, Faculty of Engineering and Science, University of Agder, N-4898 Grimstad, Norway (e-mail: peterg07@student.uia.no).

Yousef Iskandarani is with the Department of Engineering, Faculty of Engineering and Science, University of Agder, N-4898 Grimstad, Norway (e-mail: yousef.iskandarani@uia.no).

Hamid Reza Karimi is with the Department of Engineering, Faculty of Engineering and Science, University of Agder, N-4898 Grimstad, Norway (e-mail: hamidrk@uia.no).
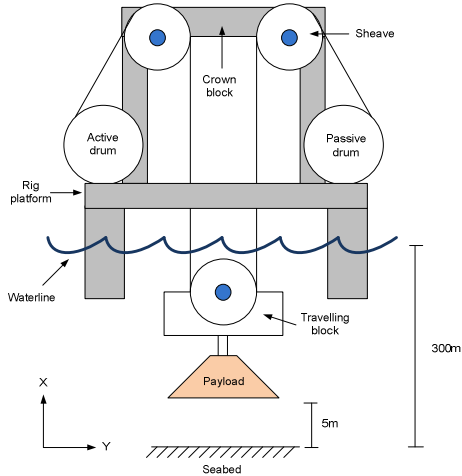
[3]. The large variation in heave compensation efficiency for different ship heave conditions is one of PHC systems' weaknesses. AHC systems on the other hand is able to adapt to varying conditions and is more accurate with an efficiency of ca. 95% [3]. Recent work on AHC systems include Neupert et al. who presented a combination of trajectory tracking disturbance decoupling controller and a prediction algorithm for an AHC system [4]. Li and Liu proposed three-degree-of-freedom dynamic models of an AHC system subject to a sinusoidal wave.

The problem at hand is the performance optimization of a virtual AHC system applied on a hoisting rig. The system as a whole must handle two load cases with a submerged payload while under the influence of a heave motion: 1. Vertical position stabilization and 2. Lowering of 5m to the seabed. Heave compensation must decrease the oscillations of the payload by at least 95%, which is the present competitive efficiency for such a system. This reduces excessive loads transferred to the wire and the rest of the hoisting machinery. The lowering time should be less than 10s and a seabed landing with no significant impact loads should be achieved.The AHC model is to be run for load case 1 and 2under the influence of a constantsinusoidal heave motion. The payload must land smoothly on the seabed to avoid large impact loads. The performance of the system must be optimized based on the simulation results.

Modeling of the AHC system require three main parts: the mechanical, hydraulic and control system.The mechanical system consists of components of the hoisting rig that are important to the overall dynamics. This includes the drums, sheaves, wire, travelling block, payload and the rig itself. The hydraulic part consists of the hydraulic circuit that actuates the mechanical system. This is also where the control elements are located: the servo valves and displacement pump. The control system regulates the hydro-mechanical system through the control elements using a controller algorithm.

II. MECHANICAL SYSTEM MODELING

The modeling and simulation of the mechanical system is based on the minimum sheave configuration of 3 sheaves. This is not necessarily the most efficient arrangement in terms of cost or performance, but its modeling process is shown in this paper due to its simplicity.Modeling and simulation of sheave configurations with more sheaves follow the same principle as that of the 3 sheave system.In the end the most cost efficient design of 7 sheaves was used and simulated. The overall mechanical system is illustrated in Fig. 1. The actual cost analysis lies outside this project's scope.

Fig. 1The hoisting rig schematic.

A. Dynamic Analysis – Linear Dynamics

Equations of motion were set up for the mechanical system. Free body diagrams and kinetic diagrams (KD's) are drawn from the payload and upwards to the active drum. The dynamic analysis takes into account:

- Friction between sheave bearing pin and sheave.
- Inertia of sheaves, drum, combined payload and wire.
- Wire dynamics: stiffness, damping, elongation and rate of elongation.
- Wire weight.
- Wire buoyancy.
- Seabed dynamics.
- Hydrodynamic drag.

Simplifications include having a constant active drum and wire mass. This is justified by the limited movement that the system goes through in load case 1 and 2. The passive drum is not in operation during the load cases, thus it is neglected and the wire to it is seen as anchored to the rig platform. The wire mass is divided into upper and lower sections. This method allows the effect of wire elongation to be shown. The lower wire section mass of wire 1 and 2 have been combined with the mass of the payload, sheave 2 and travelling block. The overall hoisting rig dynamic model schematic can be seen in Fig. 3.
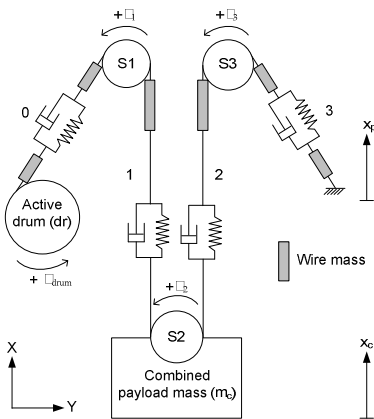

Fig. 2The hoisting rig dynamic model schematic.

Combined Payload

The payload, travelling block and travelling block sheave are combined into one mass called the combined payload. Its FBD and KD are shown in Fig. 4.
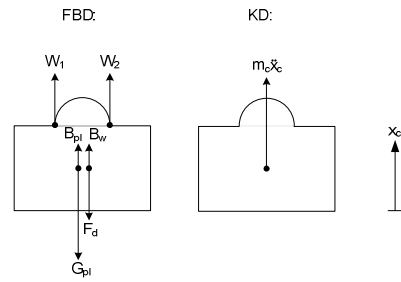

Fig. 3The FBD and KD of the combined payload.

The equivalent equation for the FBD and KD is:

$$W_1 + W_2 - \text{sign}(\dot{x}_c)\, F_d + B_w + B_{pl} - m_c g + F_{sb}{}^* = m_c \ddot{x}_c \qquad (1)$$

where the wire and payload buoyancy are $B_w = V_w g$ and $B_{pl} = V_{pl}\, g$ respectively. The drag force is $F_d = \frac{1}{2}\rho A_{pl} C_d \dot{x}_c$, where the water density is $\rho = 1027\frac{kg}{m^3}$ and the drag coefficient is assumed to be $C_d = 1,8$. The seabed force F_{sb} is modeled as a spring-damper as shown in Fig. 5.It is only in effect when the payload position x is below the seabed level. This gives $F_{sb} = k_{sb} \cdot x + c_{sb} \cdot \dot{x}$, where spring coefficient is $k_{sb} = 10^6\,\frac{N}{m}$ and damping coefficient is $c_{sb} = 10^2\,\frac{Ns}{m}$.
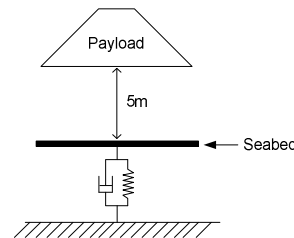

Fig. 4 Seabed dynamics.

Wire Force

The wire can be regarded as an elastic rod and therefore modeled as a spring. Damping is also added tothis model to account for internal friction in the wire. Therefore, the general wire force equation is $W = F_s + F_d$, where the spring force is derived from Hooke's law: $F_s = k\delta$.Thedamper force is $F_d = c\dot{\delta}$.The damper coefficient c is defined as 10 % of the spring coefficient. However, this is only a roughestimate and may not reflect the actual value.This gives the following for the wire forces:

$$W_0 = k_o \delta_0 + c_o \dot{\delta}_0 \qquad (2)$$
$$W_1 = k_i \delta_1 + c_i \dot{\delta}_1 \qquad (3)$$
$$W_2 = k_i \delta_2 + c_i \dot{\delta}_2 \qquad (4)$$
$$W_3 = k_o \delta_3 + c_o \dot{\delta}_3 \qquad (5)$$

Wire Elongation

The wire elongation in each wire section is determined by the difference in rotational displacement by thesheaves. In addition to this, it is known by the difference between the heave motion $z(t)$ and the motion ofthe combined payload $x(t)$. The passive drum is not in the scope of this project and thusdoes not affect the wire elongation.This gives the following equations:

$$\delta_0 = \phi_{\text{drum}} \frac{D_{drum}}{2} - \phi_1 r_1 \tag{6}$$

$$\delta_1 = \phi_1 r_1 + z(t) + \phi_2 r_2 - x(t) \tag{7}$$

$$\delta_2 = -\phi_2 r_2 + z(t) - \phi_3 r_3 - x(t) \tag{8}$$

$$\delta_3 = \phi_3 r_3 \tag{9}$$

which are valid for $\delta_n \geq 0$, but 0 for $\delta_n < 0$. This is because no wire compression (negative elongation) ismodeled. The heave motion $z(t)$ consists of a sine wave with 1m in amplitude and frequency of 0,1Hz:

$$z(t) = \sin(2 \cdot \pi \cdot f \cdot t) \tag{10}$$

Wire Rate

Wire rate in each wire section is described by the following equations:

$$\dot{\delta}_0 = \dot{\phi}_{\text{drum}} \frac{D_{drum}}{2} - \dot{\phi}_1 r_1 \tag{11}$$

$$\dot{\delta}_1 = \dot{\phi}_1 r_1 + \dot{z}(t) + \dot{\phi}_2 r_2 - \dot{x}(t) \tag{12}$$

$$\dot{\delta}_2 = -\dot{\phi}_2 r_2 + \dot{z}(t) - \dot{\phi}_3 r_3 - \dot{x}(t) \tag{13}$$

$$\dot{\delta}_3 = \dot{\phi}_3 r_3 \tag{14}$$

Wire Weight

The inner wires of the lower wire sections are seen as part of the combined payload mass, thereby having its mass and inertia modeled as part of this component. The other wire mass sections are modeled on their own, see Fig. 6.
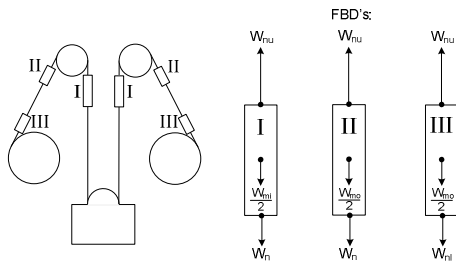

Fig. 5 FBD's of the upper inner (I), upper outer (II) and lower outer (III) wire mass sections.

The equivalent equations for the FBD's are:

$$W_{1u} - \frac{W_{mi}}{2} - W_1 = 0 \tag{15}$$

$$W_{2u} - \frac{W_{mi}}{2} - W_2 = 0 \tag{16}$$

$$W_{0u} - \frac{W_{mo}}{2} - W_0 = 0 \tag{17}$$

$$W_{3u} - \frac{W_{mo}}{2} - W_3 = 0 \tag{18}$$

$$W_0 - \frac{W_{mo}}{2} - W_{1l} = 0 \tag{19}$$

$$W_3 - \frac{W_{mo}}{2} - W_{2l} = 0 \tag{20}$$

where $W_{mi} = m_i \cdot g$ and $W_{mi} = m_o \cdot g$

Sheaves

The upper sheaves are fixed to the crown block of the drilling rig. This means they have no acceleration in relation to the overall system. Hence, no kinetic diagram is drawn for these sheaves. The FBD's of the crown block sheaves are shown in Fig. 7.
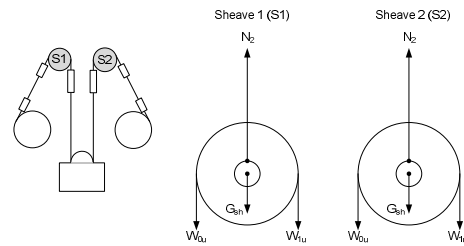

Fig. 6 FBD's of the upper sheaves.

The equivalent equations for the FBD's are:

$$N_1 - G_{sh} - W_{1l} - W_{1l} = 0 \tag{21}$$

$$N_3 - G_{sh} - W_{2u} - W_{3u} = 0 \tag{22}$$

The lower sheave (S3) moves with the combined payload giving it acceleration $\ddot{x}_c$, see Fig. 8.
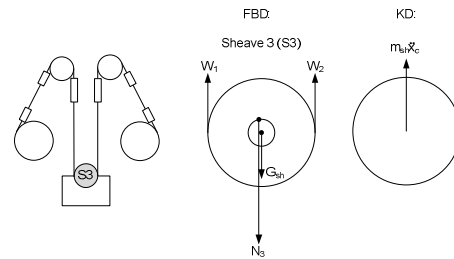

Fig. 7The FBD and KD of the lower sheave.

The equivalent equation for the FBD and KD is:

$$N_2 - G_{sh} - W_2 - W_3 = m_{sh} \ddot{x}_c \tag{23}$$

Bearing-Pin Friction

The coulomb friction equation for dry friction in the static case is used to model the bearing-pin friction: $F_f = \mu \cdot N$. This is only an approximation as the ideal case would be to model the kinetic friction. The friction between the three bearings and pins with normal forces from (21), (22) and (23)inserted are:

$$F_{f1} = \mu \cdot abs\left(G_{sh} + W_{0u} + W_{1u}\right) \tag{24}$$

$$F_{f2} = \mu \cdot abs\left(-G_{sh} + W_1 + W_2 + m_{sh}\ddot{x}\right) \tag{25}$$

$$F_{f3} = \mu \cdot abs\left(G_{sh} + W_{2u} + W_{3u}\right) \qquad (26)$$

where the friction factorbetween the bearing and pin is approximated as μ=0.1. The *abs*sign in front of the paranthesis means *absolute value*. It is used because the sign of the friction forces is to be determined by the rotational direction of the sheaves, see (27), (28) and (29).

B. Dynamic Analysis – Rotary Dynamics

Sheaves

The torque consists of the wire force times the sheave radius, see Fig. 9. Its sign is positivein the counter clockwise rotational direction.
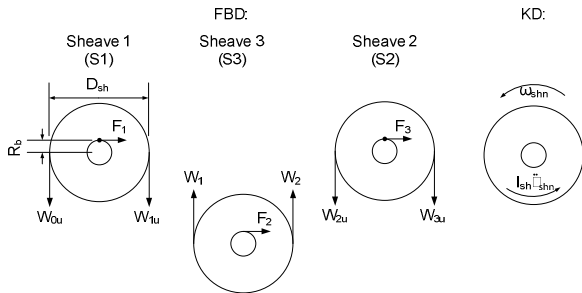

Fig. 8 FBD's and KD for the sheaves showing rotary dynamics.

Inserting the friction forces equations (24), (25) and (26) in with the equivalent equations for the FBD's and KD yields:

$$\frac{D_{sh}}{2}\left(W_{ou} - W_{1u}\right) - \text{sgn}\left(\phi_{sh}\right)N_u \cdot \mu \cdot R_b = I_{sh}\ddot{\phi}_{sh1} \qquad (27)$$

$$\frac{D_{sh}}{2}\left(-W_1 + W_2\right) - \text{sgn}\left(\phi_{sh}\right)N_u \cdot \mu \cdot R_b = I_{sh}\ddot{\phi}_{sh2} \qquad (28)$$

$$\frac{D_{sh}}{2}\left(W_{ou} - W_{1u}\right) - \text{sgn}\left(\phi_{sh}\right)N_u \cdot \mu \cdot R_b = I_{sh}\ddot{\phi}_{sh3} \qquad (29)$$

Sheave Inertia

The sheave is considered a thick walled cylinder and therefore its inertia is calculated as such:

$$I_{sh} = 0.5 \cdot m_{sh} \cdot \left[\left(\frac{D_{sh}}{2}\right)^2 - \left(\frac{D_{sh}}{2}\right)^2\right] \qquad (30)$$

Active Drum

The torque and inertia of the active drum is investigated in Fig. 10.

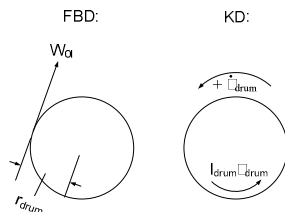

Fig. 9The FBD and KD for the active drum.

From the FBD and KD we get the following equation:

$$-W_{0l}r_{drum} = I_{drum}\ddot{\phi}_{drum} \qquad (31)$$

Active Drum Inertia

The active drum inertia I_{ad}consists of the inertia of a thick-walled cylinder and two massive disks.

$$I_{ad} = I_1 + 2 \cdot I_2 \qquad (32)$$

where $I_1 = 0.5 \cdot m_{cyl} \cdot \left[\left(\frac{d_D}{2}\right)^2 - \left(\frac{d_D}{2-h_D}\right)^2\right]$ is the inertia of the thick cylinder and inertia of the massive disk is $I_2 = 0.5 \cdot m_{DE} \cdot \left(\frac{d_{DE}}{2}\right)^2$.

III. HYDRAULIC SYSTEM MODELING

Using the steady state design approach as described by Stecki and Garbacik [6] a hydraulic circuit concept was proposed. This design method doesn't take into consideration the actual dynamics of the system, so the designed system must be verified during the simulation phase. The proposed hydraulic circuit consists of two hydraulic power units, two servo valves, a hydraulic motor, and a gearbox. Fig. 11illustrates this hydraulic circuit concept.
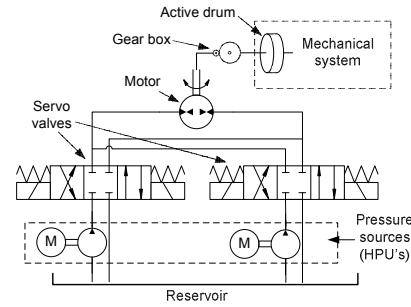

Fig. 10The hydraulic circuit concept.

A. Operating Cycle

The operating cycle defines the required motor angular velocity. Starting with the platform heave velocity which is obtained by deriving (10):

$$\dot{z}(t) = 2 \cdot \pi \cdot f \cdot \cos(2 \cdot \pi \cdot f \cdot t) \qquad (33)$$

and multiplying it with the gearing from the sheavei_{sh} and gear box i_{gear} and finally dividing it by the active drum radius yields thereference equation for the motor angular velocity for load case 1:

$$m(t) = i_{sh}\, i_{gear}\, \dot{z}(t) \qquad (34)$$

B. System Dimensioning

Gearbox

Usingthe required drum torque $\tau_{drum}$and choosing an equivalent or larger value for nominal torque τ_{2n}in a gearbox catalogue, a gearbox size can be determined. The next step is to determine the output duration factor $f_{h,required} = n_2 \cdot h_r$,where $h_r$is the life duration for the system, which is 500hours, andn_2 is the angular output speed that is equal to drum speed:

$$n_{drum} = \frac{\omega_{drum}\, 30}{\pi} \qquad (35)$$

where $\omega_{drum} = \frac{V_{drum}}{r_{drum}}$ and $V_{drum} = g_{sh} \dot{z}_{max}$

Hydraulic Motor

To determine the size of the hydraulic motor D_M, calculation of the motor discharge displacement $D_{M,min}$ is needed. The equation below is used to determine this component:

$$D_{M,min} = 10^5 \cdot 10^6 \left(\frac{2\pi \tau_M}{p_M} \right) \eta_{hmM} \qquad (36)$$

where required motor torque is: $\tau_m = \frac{\tau_{drum}}{i_{gear}}$

Once the duration factor has been calculated, one can use a data table for RR (Riduttore lineare) gearboxesto choose a reduction gear ratio that is suitable for the working conditions required: $\tau_2 \geq \tau_{drum}$ and $f_h \geq f_{h,required}$.

Servo Valves

The size and number of the servo valves is determined by the needed motor flow, Q_M:

$$Q_M = \frac{D_M n_M}{1000 \eta_{vm}} \qquad (37)$$

where n_M is the motor speed, η_{vm} is the volumetric efficiency of the motor.

Hydraulic Power Units

The pressure drop over the servo valves is 70bar. The chosen pressure level is 150bar. Thus, it was decided to choose an HPU with 260 bar since this gives an excess of:$260-150-70 = 40$ bar which can allow for potentiallybigger pressure differentials.

IV. CONTROL ARCHITECTURE

For controlling the draw-works in load case 1 and 2 a cascaded controller was used. The outer controller is a P-controller while the inner controller is a PI-controller. The main reason for using this setup is thatthe contol job is twofold: one is to heave compensate, the other is to lower the payload 5 m. Combining these two load cases could prove difficult for a single controller feedback system. Therefore, a cascaded controller is selected.
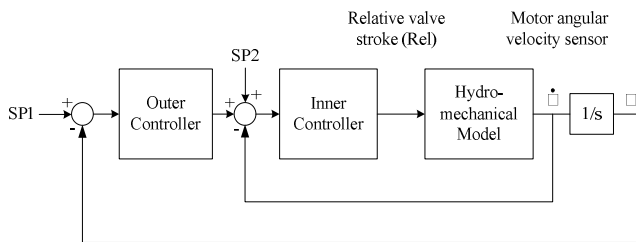

Fig. 11 The cascade control architecture for the draw-works.

The outer controller is used for positioning the payload. Therefore, its set point is in motor angular displacement. The process variable of the outer loop is the angular displacement of the motor. The output of the outer controller is added with the inner loop set point.

V. SIMULATION

The equations of motion of the mechanical system and component dimensions of the hydraulic system are implemented in *Simulation X*. Simulation results for wire force and active drum torque were gathered,see Fig. 2. The authors ran several sets of simulations for sheave configurations up to

Table II.
Comparison of Static Calculations and Simulated Results.

Datum	Symbol	3 Sh.	5 Sh.	7 Sh.	9 Sh.	11 Sh.	13 Sh
Wire force	N	40940	20960	14300	10970	8970	7640
Simulated wire force	N	45680	23480	15965	12165	9956	8624
Active drum torque	Nm	12880	5140	2660	1730	1280	1100
Simulated active drum torque	Nm	10860	4395	2473	1592	1217	939

13 sheaves with increments of 2. The simulation results are summarized in Table II.

A. Verification of Dimensions

The reason for gathering these results is because the dimensioning of the hydro-mechanical system starts with the values of the wire force and active drum torque. The values for the simulated results are taken as the system has reached equilibrium.

The simulation results are compared with the statically calculated parameters, see Table II. The results show that all statically calculated wire forces are lower than the simulated ones. Since the wire force is a significant part of dimensioning the mechanical system, it means most of the mechanical system is under dimensioned. The opposite is true for the statically calculated active drum torques, which means the hydraulic system has been over dimensioned.By adjusting the design parametersto close the gap between calculated and simulated values of wire force and active drum torque more optimized designs are achieved. The simulated values in Table II also represent the final design limits for the hydro-mechanical systems.

B. Load Case 1 and 2

Both load case 1 and 2 have been simulated for the hydro-mechanical system with 7 sheaves to verify the model.The results indicate thatthe design is within designed limits and operates satisfactorily. Fig. 15and 16show the payload displacement results for load case 1 and 2. Itcan be observed that the model stabilizes and lowers the payload gently to the desired position. A zoomed in image of load case two shows the payload position as it hits the seabed, see Fig. 17.
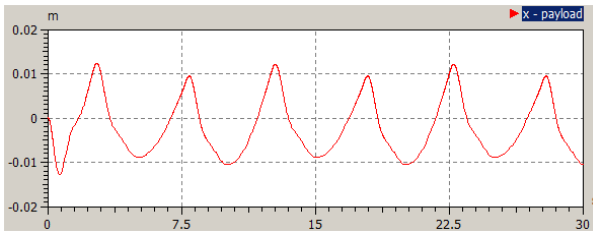
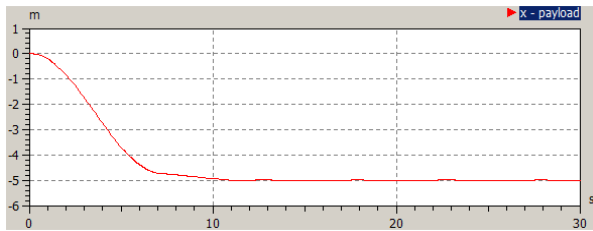Fig. 12The simulation result forload case 1 with AHC system on showing ca. ±1cm in position oscillation.

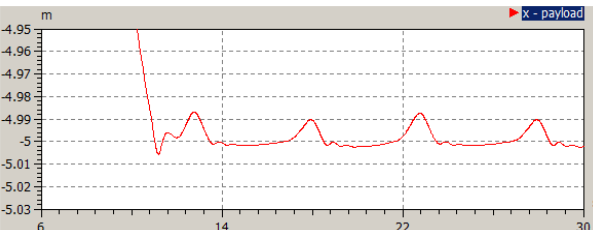Fig. 13The simulation result for payload lowering of 5m onto the seabed – load case 2.

Fig. 14A zoomed in view of payload position during load case 2.

The average wire force and active drum torque occurring during load case 2 are within the design limits, see Fig. 18 and 19. This means the system is also within limits for load case 1 because vertical position stabilization of the payload continues after the payload has been lowered. The hydraulic system also works within its limits. This is shown by Fig. 20 where the motor angular velocity reference curve overlaps the actual angular velocity.
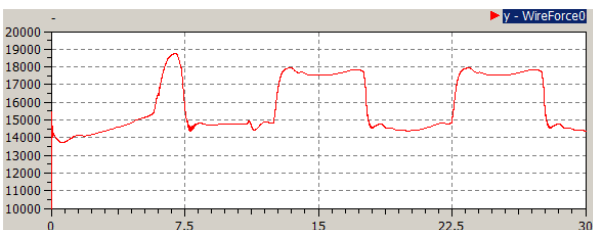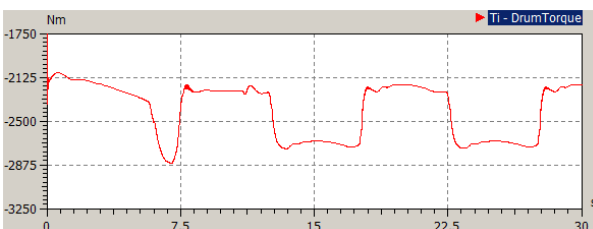

Fig. 15The simulated wire force during load case 2.

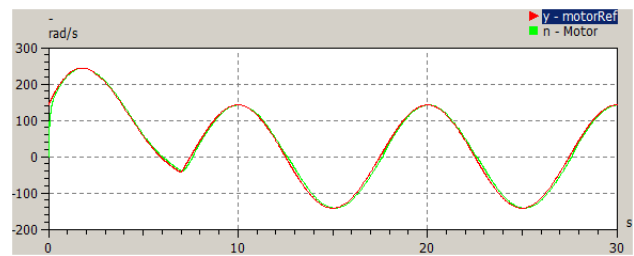Fig. 16The simulated active drum torque during load case 2.

Fig. 17The motor reference angular velocity (motorRef) and actual velocity (Motor) curves during load case 2. They are overlapping.

C. Conclusion

A simulation model of an active heave compensation system was developed for a draw-works on a hoisting rig. Importantcomponents and dynamics of the draw-works and hoisting rig were dimensioned, modeled and set up in simulation software *Simulation X.* A control architecture was set up where the controller regulates a pair of servo valves. The feedback signals were the motor angular displacement and velocity. The chosen controller algorithm was a cascaded P-PI controller which was also implemented in the simulation model. Simulations run for load case 1 and 2 showed that the hydro-mechanical system parameters are within their design limits.

VI. ACKNOWLEDGMENT

REFERENCES

[1] F. R. Driscoll, B. Buckham, and M. Nahon, "Numerical Optimization of a Cage-Mounted Passive Heave Compensation System"OCEANS 2000 MTS/IEEE Conf. and Exh. *J.*, vol. 2, no. 4, pp. 1121 - 1127, Des. 2000.
[2] J. Ni, S. Liu, M. Wang, X. Hu and Y. Dai, "The Simulation and Research on Passive Heave Compensation System for Deep Sea Mining" in *2009 Proc. IEEE Int. Conf. on Mechatronics and Automation*, pp5111 – 5116.
[3] Ocean Drilling Program. (2010, April 16). Active Heave Compensator[Online].Available:http://www-odp.tamu.edu/publi cations/tnotes/tn31/pdf/ahc.pdf
[4] J. Neupert, T. Mahl, B. Haessig, O. Sawodny, K. Schneider, "A Heave Compensation Approach for Offshore Cranes" in *Conf. Rec.* 2008 American Control Conf., pp538 – 543.
[5] L. Li, S. Liu "Modeling and Simulation of Active-Controlled Heave Compensation System of Deep-sea Mining based on Dynamic Vibration Absorber" 2009 *Proc. IEEE Int. Conf. on Mechatronics and Automation*, pp1337 – 1341.
[6] J. S. Stecki and A. Garbacik, *Design and Steady-state Analysis of Hydraulic Control Systems*. Cracow:Fluid Power Net Publications. 2002.